Deng *et al. Biochar* (2026) 8:85
https://doi.org/10.1007/s42773-026-00599-8

Biochar

ORIGINAL RESEARCH Open Access

Fungi enhance biochar and compost effects on carbon accrual in nutrient-deficient urban greenspace soils

Sihang Deng[1], Qun Gao[2*], Ling Han[3*], Xin Tong[4], Wenrui Shen[3], Anqi Liu[3], Hongkwan Lee[3], Zhencheng Ye[1], Suo Liu[1], Ke Sun[2], Xinghui Xia[2] and Yunfeng Yang[5]

Abstract

Urban greenspaces provide critical ecosystem and recreational services but are increasingly threatened by organic matter depletion, fertility decline, and nutrient cycle disruptions under rapid urbanization. Although protective measures like biochar and compost amendments are being widely implemented, their effectiveness across heterogenous urban greenspaces, and the underlying mechanisms governing these responses, remain poorly understood. In a manipulated field experiment across three urban greenspaces with contrasting intrinsic soil nutrient levels, we found that biochar and compost amendments enhanced soil carbon and nitrogen contents, with effects up to 14.4-fold stronger in nutrient-poor greenspace soils compared to nutrient-rich soils. Mechanistically, amendments in nutrient-poor sites elevated fungal diversity and the fungal-to-bacterial richness ratio, driving significant gains in soil carbon and nitrogen. In contrast, nutrient-rich sites exhibited declines in fungal diversity, network connectivity (< − 30%) and stability (− 2% to − 8%), but increased bacterial growth (> 4%) that accelerated carbon consumption, ultimately destabilizing soil carbon pools. These findings demonstrate that baseline soil nutrient status modulates amendment outcomes: in nutrient-poor soils, fungal dominance enhances carbon storage and soil fertility, whereas in nutrient-rich soils, nutrient surplus favors bacterial-driven carbon mineralization. Our study highlights fungi as pivotal drivers of soil restoration in urban greenspaces and underscores the need to prioritize nutrient-poor sites for biochar and compost interventions to maximize ecological benefits.

Highlights

- Biochar and compost amendments enhanced soil C and N storage, with effects up to 14.4-fold greater in nutrient-poor urban greenspaces than in nutrient-rich sites.
- In nutrient-poor soils, amendments increased fungal richness, and network connectivity and stability, collectively driving C and N accumulation.
- In nutrient-rich soils, amendments promoted bacterial growth but reduced the fungal-to-bacterial richness ratio, accelerating C consumption and destabilizing soil C pools.

Keywords Carbon accrual, Biochar amendment, Fungi, Functional traits, Urban greenspace

*Correspondence:
Qun Gao
gaoqun@bnu.edu.cn
Ling Han
hanling@pku.edu.cn
Full list of author information is available at the end of the article

Springer

Graphical Abstract

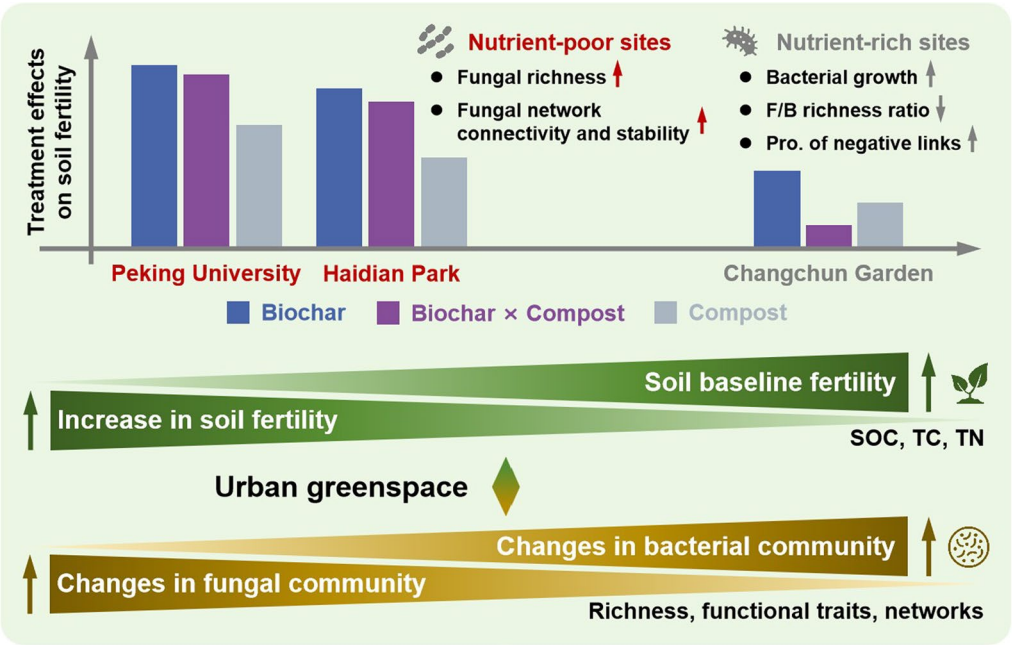

1 Introduction

Urban greenspaces, including parks and residential gardens, are anticipated to serve as the primary outdoor activity spaces for 68% of the urban population by 2050 (Delgado-Baquerizo et al. 2021). These sustainable landscapes play a crucial role in supporting diverse ecosystem functions, including soil carbon sequestration, nutrient cycling, water regulation, and plant-soil mutualisms (Charlop-Powers et al. 2016; Fan et al. 2023). Moreover, these greenspaces serve as vital habitats for a wide range of wildlife, supporting urban biodiversity by sustaining bird species (e.g., pigeons), terrestrial and arboreal mammals (e.g., squirrels), and a wide array of microorganisms (e.g., bacteria and fungi) (Delgado-Baquerizo et al. 2021; Fairbairn et al. 2024). However, the rapid pace of urbanization (Wu et al. 2023), coupled with increasing environmental and social pressures, threatens these ecosystems by depleting soil organic carbon (SOC) stocks (Guo et al. 2024), disrupting nutrient cycling (Fan et al. 2023), and promoting the proliferation of soil-borne pathogens, which pose substantial risks to both wildlife and human health (Luo et al. 2024). Therefore, implementing targeted interventions to enhance carbon sequestration and restore soil fertility is crucial for safeguarding the ecological integrity of urban greenspaces in the face of accelerating urbanization and global climate change.

Among various intervention strategies, biochar has emerged as a promising strategy for mitigating climate change (Lehmann et al. 2021). In agricultural systems, biochar application has been shown to enhance crop yields and reduce greenhouse gas emissions (Nan et al. 2025). It also enhances soil carbon sequestration by suppressing the mineralization of native carbon pools and promoting the stabilization of fresh organic inputs, often referred to as negative priming effects (Lehmann et al. 2021). Moreover, composting municipal green waste and its subsequent addition to local urban greenspaces is increasingly promoted in China as a sustainable approach to improving soil fertility and organic matter content (Reyes-Torres et al. 2018). However, the sole application of biochar is often constrained by its high production cost and the potential risk of soil nitrogen limitation due to its excessively high carbon-to-nitrogen (C/N) ratio (Tian et al. 2025). In contrast, compost application may increase N_2O emissions, soil pollution, and eutrophication in nearby aquatic systems due to nitrogen leaching (Gu et al. 2023). Hence, a combined application of biochar and compost has been proposed as a more balanced and sustainable solution for improving soil quality in agricultural landscapes (Nan et al. 2025; Zhou et al. 2025). However, a comprehensive assessment of the impacts of biochar and compost additions on soil carbon

dynamics and fertility enhancement across different urban greenspaces is still lacking.

Soil microorganisms, including bacteria and fungi, are central to carbon storage, nutrient cycling, and the maintenance of soil fertility in urban greenspaces (Delgado-Baquerizo et al. 2023; Fan et al. 2023). However, the role of microbial communities in mediating the responses of different urban greenspaces to biochar and compost additions remains largely unclear. In agricultural ecosystems, the addition of biochar and compost increases bacterial and fungal diversity, alters microbial community composition, and intensifies microbial competition, thereby indirectly influencing key soil properties such as SOC, TC, and TN (Chen et al. 2019; Dai et al. 2021). The introduction of exogenous organic matter, such as biochar or compost, may result in distinct microbial responses depending on the baseline soil conditions of each urban greenspace, thereby leading to differential effects on soil carbon sequestration and fertility enhancement. Meta-analyses in agricultural ecosystems reveal that soils with low initial SOC and TN content exhibit greater SOC and fertility enhancement compared to nutrient-rich soils (e.g., paddy soils) (Ling et al. 2025; Yang et al. 2025). This is likely because infertile soil have a greater carbon saturation deficit, promoting higher initial carbon sequestration rates and extending the time to reach a new equilibrium (Chen et al. 2024; Singh et al. 2022). However, whether such patterns persist in urban greenspaces remains poorly understood.

To assess the effects of biochar and compost additions on urban greenspaces and elucidate the underlying mechanisms, we conducted a manipulated field experiment across three representative urban greenspaces. We address the following key questions: (i) Can biochar and compost additions effectively promote both soil carbon sequestration and fertility enhancement in urban greenspaces? (ii) Do urban greenspaces with varying baseline nutrient levels exhibit consistent responses to our treatments? (iii) How do microbial communities play a role in mediating the observed responses? We hypothesize that the combined addition of biochar and compost will have the most pronounced effect on carbon sequestration and fertility enhancement compared to other treatments. We also hypothesize that this effect will be the strongest in greenspaces with higher background nutrient availability, in accordance with the "Matthew Effect" that resource abundance amplifies gains (Li et al. 2024; Merton 1968), for which soil microbial communities will regulate the magnitude of those treatment effects.

2 Materials and methods

2.1 Field site description and soil sampling

A manipulated field experiment investigating the effects of biochar and compost addition was carried out in three urban greenspaces located at Peking University (a university campus greenspace), Haidian Park (a park greenspace), and Changchun Garden (a residential area greenspace) in Beijing (39°59′N, 116°18′E), China (Fig. S1A). All sites share a mean annual temperature of 12.5 °C and a mean annual precipitation of 586.3 mm (1991–2020), according to publicly available meteorological records data. The urban greenspace soils are classified as silt loam, with the following compositions: Peking University (clay: 4.4%; silt: 62.1%; sand: 33.5%); Haidian Park (clay: 3.6%; silt: 53.5%; sand: 42.9%); and Changchun Garden (clay: 3.0%; silt: 55.7%; sand: 41.3%). Each urban greenspace comprised 4 groups: biochar addition (B), compost addition (C), combined biochar and compost addition (1:1 ratio, with a total mass equivalent to other treatments, BC), and control (CK) (Fig. S1B). Each treatment was applied to a 0.5 m × 0.5 m plot, with biochar and compost added at a rate of 1 kg m^{-2} in February 2023 (Fig. S1C), consistent with previous studies (0.8–1.2 kg m^{-2}) (Chen et al. 2019; Nan et al. 2025). Biochar with a pH of 8.4 in water and a bulk density of 0.4 g cm^{-3} was produced from kitchen waste through slow pyrolysis at 450 °C for 48 h in a closed limited-oxygen chamber. The compost was produced by decomposing garden waste (e.g., litter and fallen leaves) with the temperature maintained at 55 °C for 20 days, after which the final product achieved a germination rate of 90%. The added biochar contained 63.8% TOC, 64.7% TC, and 0.7% TN, while the added compost contained 18.6% TOC, 18.7% TC, and 1.6% TN (Table S1). To minimize anthropogenic disturbance during the experiment, informational signage was installed and regular coordination with local greenspace managers was maintained. Initial baseline soil samples were collected from control plots prior to treatment application and served as reference points for treatment effect evaluation. A total of 75 topsoil samples (3 urban greenspaces × 25 samples per greenspace) at a depth of 0–20 cm were collected at each of seven time points throughout the experiment (Fig. S1C). The mean soil temperatures recorded at each sampling time point were 0 °C, 3.5 °C, 8.9 °C, 14.5 °C, 17.0 °C, 20.5 °C, and 24.5 °C. To minimize spatial heterogeneity, each soil sample was obtained by compositing three soil cores collected using a 2.5 cm diameter soil sampler. The sampling holes were refilled with root-free soil collected from nearby soil to maintain the integrity of the experimental setup. Moreover, the refilled sites were marked to avoid repeated sampling at the same

location. Upon collection, soil samples were immediately transported to the laboratory and stored at −80 °C for subsequent analyses.

2.2 Soil physicochemical properties and CO_2 flux measurements

Volumetric soil water content (%V) was measured for each sample. Soil CO_2 flux was measured using an LI-8100A soil flux system equipped with a soil CO_2 flux chamber. After removing visible roots (>0.2 cm) and stones, soil samples were subjected to physicochemical analyses. Soil total carbon (TC) and total nitrogen (TN) were measured using a dry combustion C/N analyzer. Soil total organic carbon (SOC) was measured using the dichromate ($K_2Cr_2O_7$) oxidation-heating method. Soil nitrate (NO_3^-) and ammonium (NH_4^+) concentrations were measured by extracting soil samples with 50 mL of 2.0 mol L^{-1} potassium chloride (KCl) for 60 min, with subsequent analysis performed on a flow-injection analyzer. Soil pH was measured in a 2.5:1 water-to-soil slurry, using a calibrated pH meter equipped with a combined glass electrode. The Mo-Sb antiluminosity method (Olsen method) was employed to quantify the available phosphorus (AP) in soil. Available potassium (AK) content was determined by extracting 5.0 g of soil with 25 mL of neutral 1.0 mol L^{-1} NH_4OAc for 30 min, followed by filtration through filter paper.

2.3 DNA extraction and amplicon sequencing

Genomic DNA was extracted from 0.5 g of homogenized soil sample, using a freeze-grinding approach followed by a sodium dodecyl sulfate (SDS)-based lysis method (Zhou et al. 1996). The extracted DNA was subsequently purified using a PowerSoil DNA Isolation Kit (Majorbio, Shanghai, China), following standard procedures (Zhou et al. 1996). A two-step PCR amplification protocol with a phasing primer technique (Wu et al. 2015) was employed to construct the sequencing library. Universal primer sets were used to amplify the V4 hypervariable region of bacterial and archaeal 16S rRNA genes (515F (5′- GTGCCAGCMGCCGCGG-3′), and 907R (5′-CCG TCAATTCMTTTRAGTTT-3′)), and the fungal ITS region between the 5.8S and 28S rRNA genes (ITS5F (5′-GGAAGTAAAAGTCGTAACAAGG-3′), and ITS1R (5′-GCTGCGTTCTTCATCGATGC-3′)). To reduce batch effects, all samples from different sites, treatments, and time points were randomized prior to processing and sequenced simultaneously.

2.4 Bioinformatic analyses

Raw sequence reads were generated using the Illumina MiSeq platform (Illumina, San Diego, CA, USA) and processed via a customized sequence analysis pipeline based on the Galaxy platform (version 0.1.0) (Giardine et al. 2005). High-quality 16S rRNA gene and ITS sequences were clustered into zero-radius operational taxonomic units (zOTUs) at 100% similarity using the UNOISE3 algorithm (Edgar 2018). Notably, there were no significant differences ($p > 0.05$) in the sequencing depth across all samples (Fig. S2), ensuring analytical consistency and biological comparability. Taxonomic classification of 16S rRNA gene zOTUs was performed using the Silva Classifier (version 138.1) with a confidence cut-off of 70%. Sequences identified as archaea, chloroplasts, or mitochondria were excluded. Fungal ITS zOTUs were classified using the Ribosomal Database Project Classifier, with the UNITE Fungal ITS training set with a confidence cut-off of 70%. In addition, plant pathogenic fungi were identified through comparison with the FungalTraits database (Põlme et al. 2020), which is the most comprehensive resource available for predicting fungal functional guilds, containing trait and host information for over 90,000 fungal species. In the subsequent comparative analyses, the number of sequences in each sample was rarefied to 32,553 sequence reads for the 16S rRNA gene and 47,614 sequence reads for ITS sequences.

2.5 Statistical analyses

Various statistical analyses were conducted using R software (version 4.2.1), primarily employing the vegan package (version 2.6.4) unless otherwise specified. Microbial richness was calculated via the Picante package in R software (Kembel et al. 2010). To account for the repeated measures in the dataset, linear mixed-effects models (LMMs) were applied to evaluate the treatment effects and differences among urban greenspaces using lme4 package in R software (Bates et al. 2015). Wald type II χ^2 tests were used to calculate *p*-values from the LMMs based on the car package in R software. Differences in treatment effect sizes among three urban greenspaces were examined using a post-hoc least significant difference (LSD) test following one-way repeated-measures ANOVA. Permutational multivariate analysis of variance (Adonis) was employed to assess treatment-induced shifts in microbial communities based on Bray–Curtis dissimilarity matrices. Non-metric multidimensional scaling (NMDS) was performed to visualize the clustering of microbial communities. Correlation coefficients (r^2), slopes, and *p*-values were calculated using Pearson correlation. To account for multiple comparisons, all *p*-values were adjusted using the false discovery rate (FDR) correction.

The rRNA operon (*rrn*) copy numbers for bacterial zOTUs were estimated using the *rrn*DB database (Dai et al. 2022; Lee et al. 2009) (version 5.9, https://rrndb.umms.med.umich.edu/downloads/, detailed in

Supplementary Method S1). The niche breadth was used to quantify habitat specialization and was calculated for bacterial and fungal zOTUs within each urban greenspace based on Levins' method (Levins 1968). To classify microbial ecological strategies, we identified microbial generalists and specialists by calculating zOTU occurrences through 1,000 simulated permutations using the quasiswap permutation algorithm implemented in the EcolUtils R package (detailed in Supplementary Method S2) (Salazar 2015).

Microbial co-occurrence networks were constructed using relative abundance datasets of bacterial and fungal zOTUs. Given the temporal nature of the dataset, local similarity analysis (LSA) was used to identify time-dependent associations among microbial taxa (Ruan et al. 2006), which enables the construction of association networks from a time series dataset containing a single observation per time point (detailed in Supplementary Method S3) (Weiss et al. 2016). Using the igraph package in R software (Csardi and Nepusz 2006), we calculated the topological properties of microbial networks (detailed in Supplementary Method S3). The stability of each microbial network was assessed through simulated random species removal (Montesinos-Navarro et al. 2017). Moreover, we quantified network natural connectivity after random node removal (Wu et al. 2010), which serves as a complementary metric for assessing the robustness of complex networks (detailed in Supplementary Method S3).

To quantify the relative importance of stochasticity, we calculated the modified stochasticity ratio (MST) based on a standard null-model algorithm using Bray–Curtis taxonomic metrics (detailed in Supplementary Method S4) (Ning et al. 2019). To investigate the relationships between background soil physicochemical properties, microbial community responses, and changes in environmental factors across three urban greenspaces, Partial least squares path modeling (PLS-PM) analysis was performed using the plspm package in R software (Sanchez 2013) as PLS-PM is well-suited for estimating cause-effect relationships with small sample sizes (detailed in Supplementary Method S5). To correct for potential temporal autocorrelation, background environmental factor values were averaged across different sampling time points under different treatment conditions within each urban greenspace.

3 Results

3.1 Baseline soil physiochemical properties in responses to treatments

Baseline values of soil organic carbon (SOC) varied substantially among the three urban greenspaces ($p < 0.001$; Fig. S3), with the lowest content observed in greenspaces of Peking University (0.58 ± 0.16%) and the intermediate content at Haidian Park (0.88 ± 0.13%), while Changchun Garden showed the highest content (1.97 ± 0.33%). Similar patterns were observed for soil total carbon (TC, $p < 0.01$) and total nitrogen (TN, $p < 0.005$; Fig. S3). Ammonium nitrogen (NH_4^+) content did not differ significantly among three sites (Fig. S3), but nitrate (NO_3^-) content at Peking University was significantly lower ($p < 0.02$) than those at Haidian Park and Changchun Garden (Fig. S3). Soil water content at Changchun Garden was significantly lower than those at Peking University and Haidian Park (Fig. S3). Available phosphorus (AP) and available potassium (AK) levels were also significantly lower ($p < 0.04$) at Peking University compared to Changchun Garden (Fig. S3). No significant differences were observed in soil pH and CO_2 flux among three urban greenspaces (Fig. S3). Collectively, these results characterize the greenspace soil at Peking University as a nutrient-poor environment, Changchun Garden as nutrient-rich, and Haidian Park as intermediate.

After the addition of biochar and compost in three urban greenspaces, the increase in SOC content (measured as effect size) was significantly lower at Changchun Garden than in the other two greenspaces ($p < 0.05$; Fig. 1A). Neither compost alone (effect size $\beta = 0.689$, $p = 0.264$) nor the combined treatment ($\beta = 0.095$, $p = 0.798$) led to a significant increase in SOC content at Changchun Garden (Fig. 1A). Unexpectedly, the combined treatment even reduced soil TC and TN contents at Changchun Garden ($\beta = -1.103$ to -0.794, $p < 0.01$; Fig. 1B, C). Across all three sites, Changchun Garden exhibited the weakest response in TC and TN enhancement ($p < 0.05$; Fig. 1B, C). Apart from a significant increase in NO_3^- content by compost addition at Changchun Garden ($\beta = 0.802$, $p = 0.004$), no treatment had significant effects on soil NH_4^+, NO_3^-, water content, or pH at any site (Fig. S4A–D). Notably, biochar or compost addition significantly increased AP and AK contents at Haidian Park and Changchun Garden ($\beta = 0.993$ to 1.669, $p < 0.03$), while no such changes were observed at Peking University (Fig. S4E, F). However, the magnitude of AP and AK enhancement did not significantly differ across the three sites (Fig. S4E, F). A notable exception occurred at Haidian Park, where compost alone ($\beta = 0.765$, $p = 0.003$) and the combined treatment ($\beta = 0.770$, $p = 0.003$) significantly increased soil CO_2 flux, potentially undermining long-term carbon sequestration (Fig. 1D). Given the observed responses in soil physicochemical properties and functional process across treatments and sites, we identified SOC, TC, TN, and soil CO_2 flux as key environmental factors for subsequent analyses, which are also crucial for evaluating the effectiveness and sustainability of soil amendment strategies.

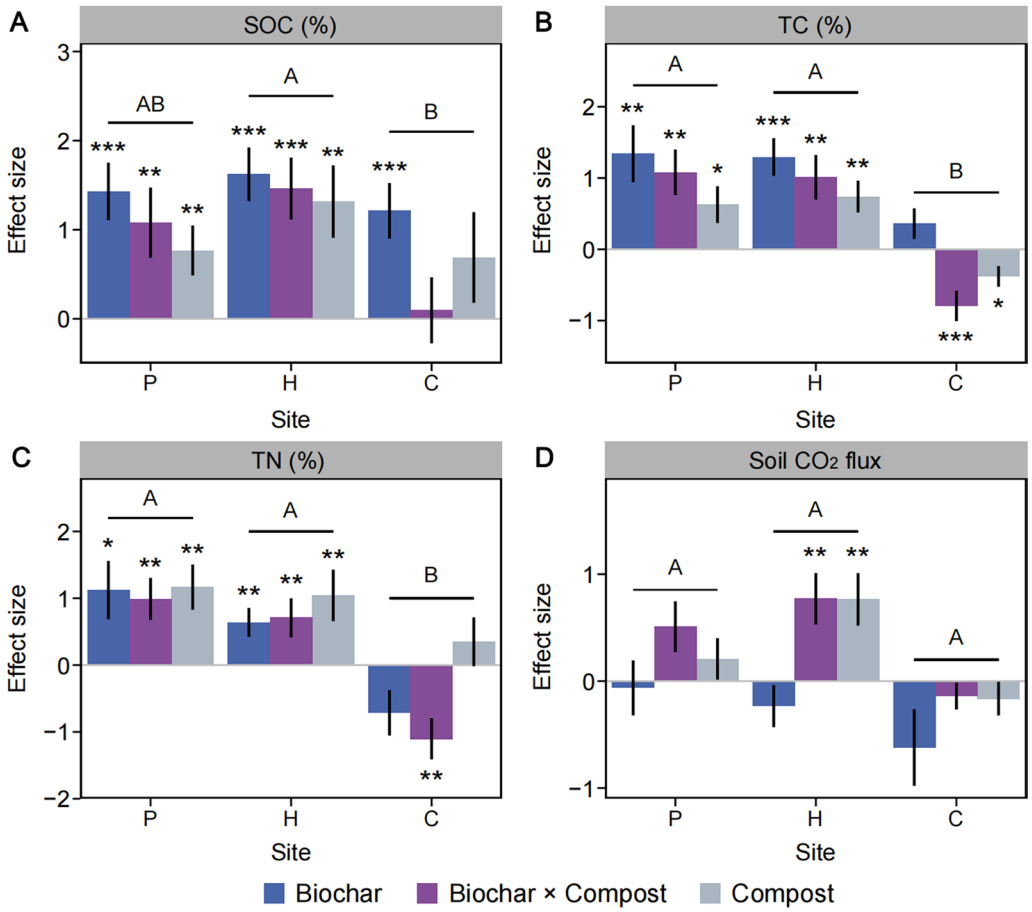

Fig. 1 Effects of single and combined treatments of biochar and compost on soil nutrient content and CO_2 flux. **A** Soil organic carbon (SOC). **B** Soil total carbon (TC). **C** Soil total nitrogen (TN). **D** Soil CO_2 flux. Effect sizes are represented as regression coefficients derived from rescaled response variables (mean = 0, standard deviation = 1) in linear mixed-effects models. Bars indicate the mean ± s.e.m. of the effect sizes. Statistical significance was determined using Wald type II χ^2 tests with false discovery rate adjustment (n = 14, soil CO_2 flux: n = 12). Significance levels are denoted as: ***$p < 0.001$, **$p < 0.01$, *$p < 0.05$. Differences in effect sizes among the three urban greenspaces were assessed using a post-hoc LSD test following one-way ANOVA (n = 9), and are indicated by uppercase letters. P: Peking University; H: Haidian Park; C: Changchun Garden

3.2 Link the changes in environmental factors to microbial community and diversity

Among the key environmental variables examined, only soil CO_2 flux showed a significant correlation between its mean values and treatment effect sizes across three urban greenspaces ($r^2 = 0.977$, $p < 0.001$; Fig. S5). Given the critical role of soil microorganisms in supporting multiple functions of urban greenspaces, such as organic matter decomposition, nutrient cycling, and plant-soil interactions (Delgado-Baquerizo et al. 2023; Fan et al. 2023), microbial dynamics may underpin the varying responses of urban greenspaces to our treatments. To test it, we analyzed bacterial (73,811 ± 29,675 reads per sample), and fungal communities across all samples (78,623 ± 27,404 reads per sample) (Fig. S2). Sequencing depths were similar among three urban greenspaces or different treatments, ensuring comparability of diversity metrics (Fig. S2). Non-parametric multivariate statistical analysis (Adonis) revealed significant differences ($p < 0.02$) in bacterial and fungal community compositions among different treatments (Table S2). Sampling site and time also influenced microbial community composition ($p < 0.01$; Table S2). The sampling site exhibited the highest explanatory power ($r^2 > 0.25$) compared to other variables ($r^2 < 0.10$; Table S2), indicating strong spatial variability of treatment effects on microbial communities. Site-specific analyses revealed that treatments significantly ($p < 0.05$) altered bacterial and fungal community compositions at Haidian Park and Changchun Garden, whereas no significant changes were detected at Peking University (Fig. S6), potentially contributing to site-level differences in soil physicochemical properties (Fig. 1).

The compost addition reduced bacterial richness compared to control at both Peking University ($\beta = -0.853$,

$p = 0.015$) and Haidian Park ($\beta = -0.777$, $p = 0.078$), and the combined treatment also reduced bacterial richness at Haidian Park ($\beta = -0.843$, $p = 0.041$; Fig. 2A). In contrast, neither treatments altered bacterial richness at Changchun Garden (Fig. 2A). Compost alone and the combined treatment reduced fungal richness at Changchun Garden ($\beta = -0.936$ to -0.687, $p < 0.03$), while the combined treatment led to a marginal increase in fungal richness at Peking University ($\beta = 0.878$, $p = 0.073$; Fig. 2B). The fungal/bacterial richness ratio (Fig. 2C) increased at Peking University ($\beta = 0.938$ to 1.016, $p < 0.02$), but decreased at Changchun Garden ($\beta = -0.945$ to -0.622, $p < 0.01$) under compost alone and the combined treatment. Among sites, the greatest decline in fungal richness occurred at Changchun Garden, while this site was least affected in terms of bacterial richness ($p < 0.05$; Fig. 2A, B). As a result, Changchun Garden exhibited the highest reduction in fungal/bacterial richness ratio ($p < 0.05$; Fig. 2C).

The effect size of treatment on bacterial richness was negatively correlated with those on TN (slope = −1.529, $p = 0.007$), while the effect sizes of treatment on fungal richness and fungal/bacterial richness ratio were positively correlated with those on TC and TN (slope = 0.699 to 1.108, $p < 0.05$; Fig. 2D − F, and Table S3). Additionally, the effect size of treatment on soil CO_2 flux was negatively correlated with those on bacterial richness (slope = −0.939, $p = 0.003$; Fig. 2D), but positively correlated with those on fungal/bacterial richness ratio (slope = 0.486, $p = 0.027$; Fig. 2F), indicating that the treatments may stimulate soil CO_2 emissions (Fig. 1D). No significant correlation was observed between the effect sizes on SOC and microbial richness (Fig. 2D − F, and Table S3).

3.3 Key microbial taxa associated with environmental responses

Different microbial lineages may vary in their responses to biochar and/or compost addition, leading to changes in key environmental factors. At the phylum level, Proteobacteria, Actinobacteriota, and Acidobacteriota dominate the bacterial communities in urban greenspaces, collectively accounting for > 60% of relative abundance and ~ 50% of species richness (Fig. S7A). The fungal communities are composed of Agaricomycetes, Mortierellomycetes, and Sordariomycetes at the class level, which contribute to > 25% of both relative abundance and species richness (Fig. S7B). Microbial lineages exhibiting significant ($p < 0.05$) treatment-by-site interactions in species richness, including Chloroflexi and Nitrospirota within bacterial community and nearly all fungal classes except for Dothideomycetes (Fig. 3A, B, and Table S4). Several microbial lineages were correlated with changes in soil physicochemical properties (Fig. 3C, D, and Table S5). For instance, changes in Chloroflexi richness were negatively correlated with those in TN and soil CO_2 flux (slope = −1.443 to −0.767, $p < 0.06$; Fig. 3C, and Table S5). Leotiomycetes, which exhibited the greatest positive effect sizes in species richness at Changchun Garden ($p < 0.05$; Fig. 3B, and Table S4), was negatively correlated with changes in TC and TN (slope = −1.500 to −1.178, $p < 0.05$; Fig. 3D, and Table S5). In contrast, Agaricomycetes, which showed the greatest decline in species richness at Changchun Garden (Fig. 3B, and Table S4), was positively correlated with changes in TC and TN (slope = 0.838 to 0.860, $p < 0.055$; Fig. 3D, and Table S5). The effect sizes of treatment on the relative abundance of specific microbial taxa (e.g., RCP2-54 and Leotiomycetes) also varied significantly ($p < 0.05$) across urban greenspaces, and were correlated with soil physicochemical property changes (Fig. S8, and Table S6). Interestingly, changes in the relative abundance of bacterial taxa were primarily correlated with TC (e.g., RCP2-54), while those in fungal taxa were correlated with multiple soil parameters, including SOC, TC, and TN (Fig. S8, and Table S6). Changes in the relative abundance of Leotiomycetes showed a significantly negative correlation with SOC and TC changes (slope = −1.136 to −0.677, $p < 0.05$; Fig. S8, and Table S6).

3.4 Microbial functional traits

Microbial responses to treatments rely on microbial life history strategies, which could be inferred by functional traits (Dai et al. 2022). Among them, the ribosomal RNA gene operon (*rrn*) copy number is a proxy for bacterial growth rate and nutrient utilization efficiency (Dai et al. 2022; Roller et al. 2016). Accordingly, we found that all three treatments increased community-level *rrn* copy number only at Changchun Garden ($\beta = 0.799$ to 1.320, $p < 0.03$; Fig. 4A). Moreover, the effect sizes of treatment on *rrn* copy number were negatively correlated with those on SOC and TC (slope = −1.257 to −0.653, $p < 0.04$; Fig. 4E, and Table S7), suggesting that accelerated microbial growth could counteract nutrient accumulation, particularly in nutrient-rich urban greenspaces. The increase in *rrn* copy number at Changchun Garden was accompanied by a decrease in the mean niche width of bacterial species under compost alone and the combined treatment ($\beta = -0.946$ to -0.569, $p < 0.03$; Fig. 4B). Additionally, the effect sizes of treatment on mean niche width were positively correlated with those on TC and TN (slope = 1.446 to 1.684, $p < 0.01$; Fig. 4F, and Table S7). Classification of bacterial species into generalists, specialists, or neutral species based on permuted niche width (Wilson and Hayek 2015) revealed a significant decline in the proportion of bacterial generalists at Changchun Garden under biochar alone and the combined treatment

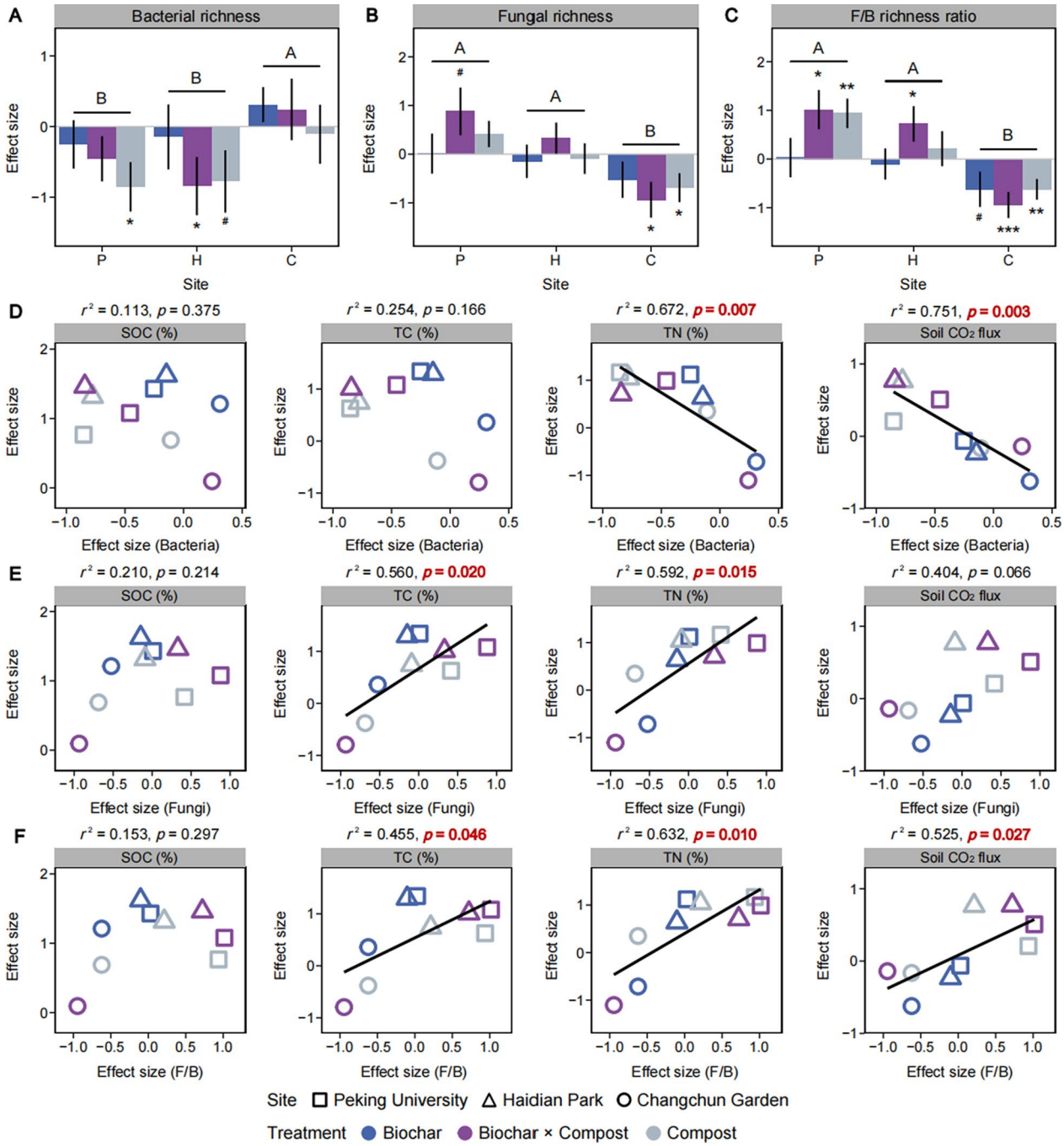

Fig. 2 Effects of single and combined treatments of biochar and compost on soil microbial communities. **A** Bacterial richness. **B** Fungal richness. **C** Fungal/bacterial (F/B) richness ratio. Effect sizes are represented as regression coefficients derived from rescaled response variables (mean = 0, standard deviation = 1) in linear mixed-effects models. Bars indicate the mean ± s.e.m. of the effect sizes. Statistical significance was determined using Wald type II χ^2 tests (n = 14). Significance levels are denoted as: ***$p < 0.001$, **$p < 0.01$, *$p < 0.05$, $^{\#}p < 0.1$. Differences in effect sizes among the three urban greenspaces were assessed using a post-hoc LSD test following one-way ANOVA (n = 9), and are indicated by uppercase letters. P: Peking University; H: Haidian Park; C: Changchun Garden. **D**–**F** Relationships between the effect sizes of the treatment on key environmental factors, and bacterial richness, fungal richness, and fungal/bacterial (F/B) richness ratio. Key environmental factors include SOC, TC, TN, and soil CO_2 flux. Pearson correlation coefficients (r^2) and p values were calculated (n = 9), with significant relationships ($p < 0.050$) highlighted in red bold text and the corresponding fitting lines are provided. Different shapes represent different urban greenspaces, while different colors represent different treatments

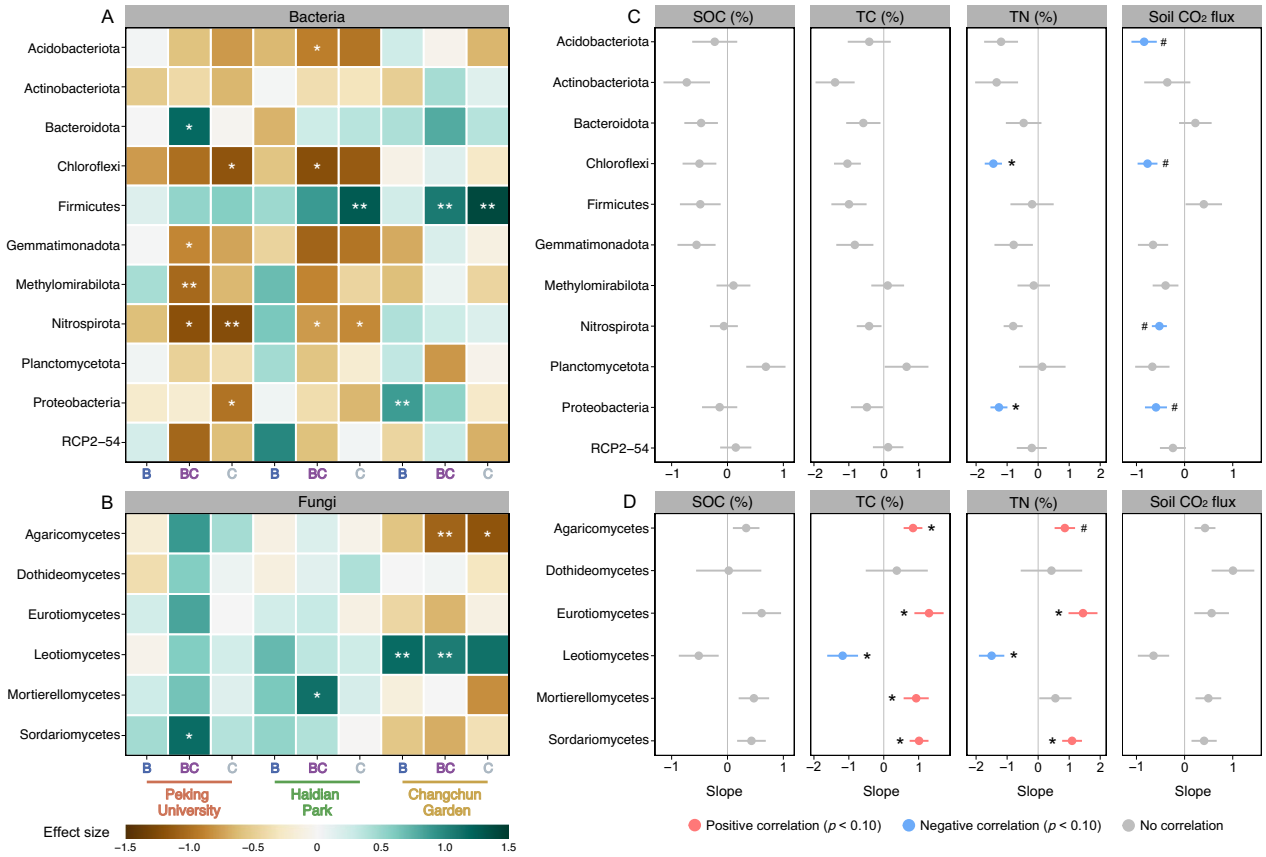

Fig. 3 Divergent responses of various microbial groups to different treatments in three urban greenspaces, and the correlation between these responses and the degree of changes in key environmental factors. **A**, **B** Treatment effect sizes on the species richness of bacterial (phylum level) and fungal (class level) communities in three urban greenspaces. Effect sizes are represented as regression coefficients derived from rescaled response variables (mean = 0, standard deviation = 1) in linear mixed-effects models. The color gradient of each box corresponds to the effect size. Statistical significance is determined using Wald type II χ^2 tests with false discovery rate adjustment (n = 14). **C**, **D** Relationships between the effect size of the treatment on key environmental factors (SOC, TC, TN, and soil CO_2 flux), and the species richness of bacterial and fungal lineages. Slopes and *p*-values with false discovery rate adjustment were calculated based on Pearson correlation (n = 9). The red circle indicates a positive correlation, the blue circle indicates a negative correlation, and the gray circle indicates no correlation. Significance levels are denoted as $^{**}p < 0.01$, $^{*}p < 0.05$, $^{\#}p < 0.1$. B: Biochar; BC: Biochar × Compost; C: Compost

($\beta = -0.646$ to -0.296, $p < 0.04$; Fig. S9A). Moreover, the effect sizes of treatment on the proportion of generalists exhibited a positive correlation with those on TN (slope = 3.029, $p = 0.012$; Fig. S9A, and Table S7), further supporting the linkages between microbial functional traits and nutrient dynamics.

The species richness of plant pathogenic fungi, as identified through the FungalTraits database (Põlme et al. 2020), varied significantly ($p < 0.05$) in response to different treatments across urban greenspaces (Fig. 4C). Richness of plant pathogenic fungi increased at Peking University under the combined treatment ($\beta = 1.114$, $p = 0.014$), but decreased at Changchun Garden under biochar addition ($\beta = -0.791$, $p = 0.03$; Fig. 4C). Moreover, the effect sizes of treatment on plant pathogenic fungal richness were positively correlated with those on TC and TN (slope = 0.905 to 1.151, $p < 0.04$; Fig. 4G, and Table S7), suggesting that higher plant pathogenic fungal richness may inhibit plant nutrient uptake, thereby promoting soil nutrient accumulation. Unlike bacterial niche responses (Fig. 4B), the mean niche width of fungal species increased at Changchun Garden under the combined treatment ($\beta = 0.695$, $p = 0.026$; Fig. 4D). However, its effect size was negatively correlated with those on TC and TN (slope = -2.464 to -1.968, $p < 0.025$; Fig. 4H, and Table S7). Similarly, the proportion of fungal specialists increased under compost alone and the combined treatment at Changchun Garden ($\beta = 0.845$ to 1.038, $p < 0.001$), and showed negative correlations with changes in TC and TN (slope = -1.385 to -1.360, $p < 0.04$; Fig. S9E, and Table S7).

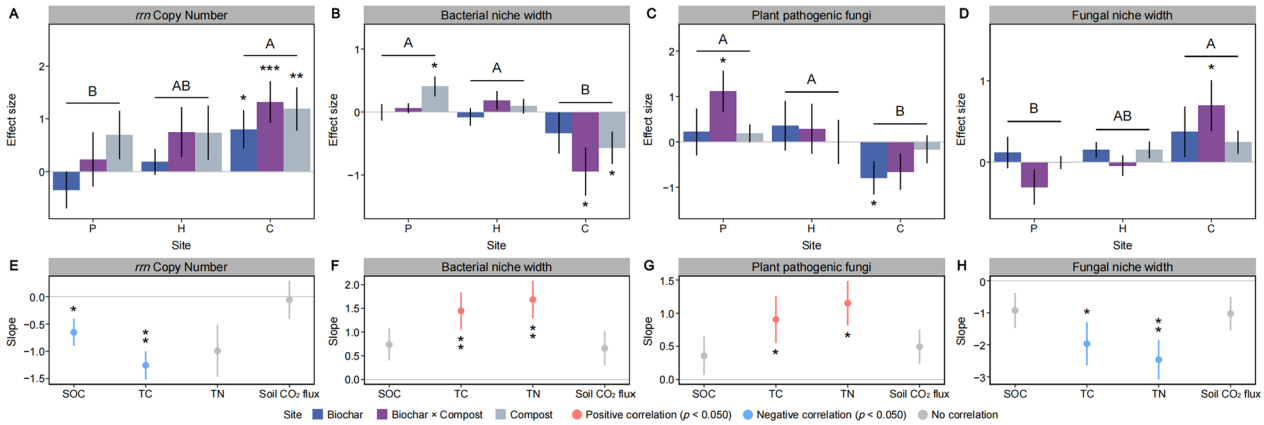

Fig. 4 Effects of single and combined treatments of biochar and compost on soil microbial functional traits. **A**–**D** Treatment effect sizes on *rrn* copy number and average unweighted niche width of the bacterial community, the species richness of plant pathogenic fungi, and the average unweighted niche width of the fungal community in three urban greenspaces. Effect sizes are represented as regression coefficients derived from rescaled response variables (mean = 0, standard deviation = 1) in linear mixed-effects models. Bars indicate the mean ± s.e.m. of the effect sizes. Statistical significance was determined using Wald type II χ^2 tests (n = 14). Differences in effect sizes among the three urban greenspaces were assessed using a post-hoc LSD test following one-way ANOVA (n = 9), and are indicated by uppercase letters. **E**–**H** Relationships between the effect size of the treatment on key environmental factors (SOC, TC, TN, and soil CO_2 flux), and the above microbial functional traits. Slopes and *p*-values were calculated based on Pearson correlation (n = 9). The red circle indicates a positive correlation, the blue circle indicates a negative correlation, and the gray circle indicates no correlation. Significance levels are denoted as ***$p < 0.001$, **$p < 0.01$, *$p < 0.05$. P: Peking University; H: Haidian Park; C: Changchun Garden

3.5 Microbial co-occurrence networks

To investigate how biochar and compost treatments influence microbial interactions over time, we employed local similarity analysis (LSA) to construct time-resolved microbial networks (Ruan et al. 2006; Weiss et al. 2016). All empirical microbial networks significantly deviated from random networks ($p < 0.01$) and exhibited scale-free features (Broido and Clauset 2019), as evidenced by their power-law distribution ($p < 0.01$; Tables S8 and S9). In bacterial networks, the total number of nodes decreased modestly at Changchun Garden across treatments relative to the control (−2.5% to 2.5%), whereas decreases were more pronounced at Peking University (−13.8% to −4.6%, $p = 0.072$; Fig. 5A, and Table S8). In contrast, fungal networks exhibited a more substantial decrease in node numbers at Changchun Garden (−25.1% to −14.0%) compared to those at Peking University and Haidian Park (−9.3% to 33.5%, $p < 0.035$; Fig. 5B, and Table S9), consistent with the observed changes in microbial richness (Fig. 2A, B). The total number of links in fungal networks decreased most at Changchun Garden compared to the control (−60.7% to −43.1%, $p < 0.04$). alongside a notable rise in the proportion of negative links (15.6% to 94.4%, $p = 0.035$; Fig. 5B, and Table S9). In contrast, Peking University exhibited a decline in negative interactions (−58.8% to −18.6%, Fig. 5B, and Table S9), suggesting that the addition of biochar and compost might intensify microbial resource competition in nutrient-rich urban greenspaces. Compared to the control, the decline in average connectivity (average links per node, average *K*) and average clustering coefficient (average CC) in fungal networks were more pronounced at Changchun Garden ($p < 0.07$; Fig. 5B, and Table S9), while bacterial networks at Changchun Garden exhibited the highest positive relative change in average CC (1.1% to 1.8%, $p < 0.1$; Fig. 5A, and Table S8). The positive relative change in modularity of fungal networks (8.0% to 19.5%) was also the highest at Changchun Garden ($p < 0.05$; Fig. 5B, and Table S9), which may be attributed to the reduced network connectivity leading to more modules.

To evaluate the effects of treatments on microbial network stability across three urban greenspaces, we simulated species extinction and quantified network robustness (Montesinos-Navarro et al. 2017; Yuan et al. 2021) (i.e., resistance to node loss) along with the natural connectivity (Wu et al. 2010) of the remaining microbial networks. The relative changes in bacterial network robustness and natural connectivity under different treatments did not differ significantly among the three urban greenspaces (Fig. 5C, and Table S10). In contrast, fungal network robustness exhibited a negative relative change under all treatments at Changchun Garden compared to the control (−7.6% to −1.8%; Fig. 5D, and Table S10), likely driven by reductions in network size (i.e., number of nodes and links) and connectivity (Fig. 5B). This decline was significantly different from the positive relative changes observed at Peking University and Haidian Park (1.5% to 8.9%, $p < 0.05$; Fig. 5D, and Table S10).

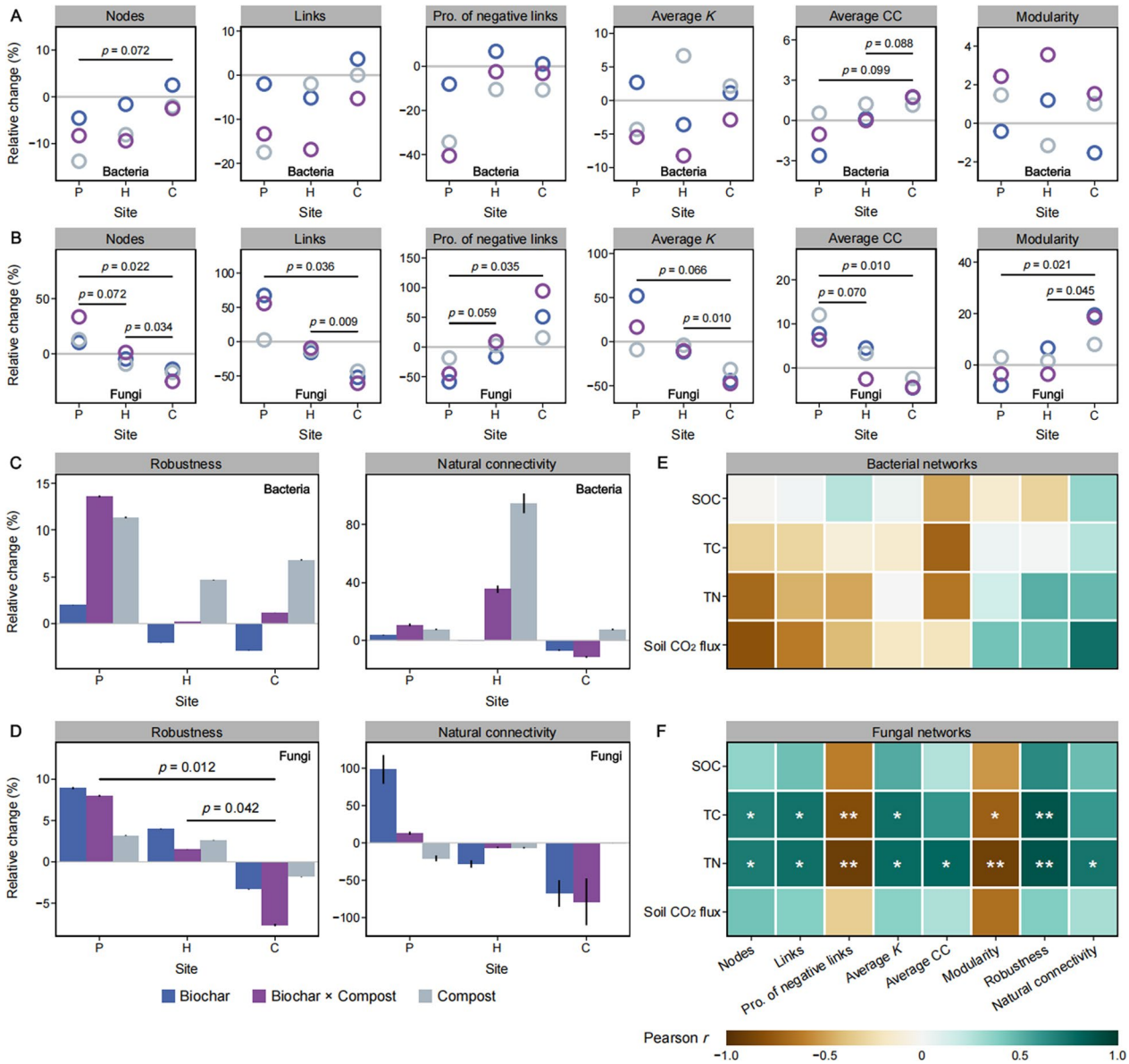

Fig. 5 Effects of single and combined treatments of biochar and compost on soil microbial network properties. **A**, **B** Relative changes in topological properties of bacterial and fungal networks under three treatments compared to the control across three urban greenspaces. Network topological properties include node and link numbers, proportion of negative links (Pro. of neg. links), average connectivity (Average *K*), average clustering coefficient (Average CC), and modularity (see Tables S2 and S3 for details). **C**, **D** Relative changes in stability indices of bacterial and fungal networks under three treatments compared to the control across three urban greenspaces. Network stability indices, including robustness and natural connectivity, were assessed after the random removal of 10% of taxa from each empirical network (see Table S11 for details). Error bars represent the mean ± standard deviation of relative changes derived from 100 simulation replicates. Differences in relative changes of network properties among three urban greenspaces were assessed using unpaired *t*-tests, with only significant differences ($p < 0.100$) displayed. **E**, **F** Relationships between the effect size of the treatment on key environmental factors (SOC, TC, TN, and soil CO_2 flux), and the relative changes in bacterial and fungal network properties. Pearson correlation coefficients (*r*) and *p*-values with false discovery rate adjustment were calculated (n = 9). Darker green indicates a significant positive correlation, while darker yellow indicates a significant negative correlation. Significance levels are denoted as: $^{**}p < 0.05$, $^{*}p < 0.1$. P: Peking University; H: Haidian Park; C: Changchun Garden

Changes in the topological properties and stability indices of microbial networks may further influence ecosystem functioning processes (Long et al. 2025; Yuan et al. 2021). Accordingly, changes in fungal networks, rather than bacterial networks, exhibited significant correlations with the effect sizes of treatments on environmental

factors (Fig. 5E, F, and Table S11). For instance, changes in the proportion of negative links in fungal networks were negatively correlated with the effect sizes of treatments on TC and TN across three urban greenspaces (slope = −1.596 to −1.300, $p < 0.04$), while increased fungal network robustness was positively correlated with higher positive treatment effects on TC and TN (slope = 12.325 to 13.758, $p < 0.02$). Changes in node and link numbers, average connectivity, and modularity in fungal networks also influenced soil TC and TN accumulation in urban greenspaces ($p < 0.1$). However, no fungal network properties were significantly correlated with the effect sizes of treatments on SOC and soil CO_2 fluxes (Fig. 5F, and Table S11).

3.6 Underlying ecological mechanisms

Microbial community composition shifts are driven by both stochastic and deterministic processes in community assembly (Ning et al. 2019). To quantify the relative contributions of these processes, we calculated modified stochastic ratios (MST) (Liang et al. 2020; Ning et al. 2019), using 50% as the threshold distinguishing the dominance of stochastic or deterministic processes. Overall, bacterial community assembly was dominated by stochastic processes across all urban greenspaces (70.9% to 87.1%; Fig. 6A). In contrast, fungal community assembly was governed by deterministic processes (30.4% to 48.4%; Fig. 6B), except biochar alone (60.3 ± 16.8%), and the combined treatment (66.3 ± 22.3%) at Changchun Garden, as well as biochar alone (56.7 ± 30.0%) at Haidian Park. Compared to the control, the proportion of deterministic processes in bacterial community assembly decreased at Haidian Park and Changchun Garden under compost alone and the combined treatment ($\beta = -0.745$ to −0.483, $p < 0.055$; Fig. 6C). Similarly, the proportion of deterministic processes in fungal community assembly decreased under biochar alone and the combined treatment at Changchun Garden ($\beta = -0.892$ to −0.765, $p < 0.01$), as well as under biochar alone at Haidian Park ($\beta = -0.442$, $p = 0.035$; Fig. 6D). Notably, the effect sizes of treatments on deterministic processes in fungal, but not bacterial, community assembly exhibited a positive correlation with their effect sizes on TN (slope = 1.449, $p = 0.014$; Fig. S10), suggesting the critical role of fungal community in regulating urban greenspace responses to treatments.

To disentangle the direct and indirect effects of soil microbial community on the variations in environmental factors, partial least squares path modeling (PLS-PM) analysis was performed with the presumed relationships (Fig. S11) among the selected subsets of soil physicochemical properties and CO_2 flux, and microbial variables (Fig. 6E, and Table S12 and S13). We found that soil physicochemical properties were positively correlated with the effect sizes of treatments on bacterial community richness (standardized path coefficient, $b = 0.861$, $p = 0.003$), but negatively correlated with those on fungal community richness ($b = -0.784$, $p = 0.012$; Fig. 6E), consistent with observed declines in fungal diversity in nutrient-rich urban greenspaces (Fig. 2B). Furthermore, the effect size of treatment on bacterial and fungal community richness was positively correlated with those on fungal functional traits, including plant pathogen and niche width ($b = 0.773$ to 0.935, $p < 0.02$; Fig. 6E), which in turn strongly influenced fungal network properties ($b = 0.855$, $p = 0.003$). No such relationship was observed in bacterial community (Fig. 6E). Collectively, the treatment effects on soil fertility (SOC, TC, and TN) and soil functioning process (CO_2 flux) were primarily mediated through bacterial diversity ($b = -0.541$, $p = 0.005$), bacterial network

(See figure on next page.)

Fig. 6 Mechanisms of microbial community assembly, and relationships between changes in microbial community and environmental responses in urban greenspaces under biochar and compost additions. **A**, **B** Bacterial and fungal community assembly processes delineated by the relative contributions of stochastic and deterministic processes. The relative contributions were quantified using modified stochastic ratios based on Bray–Curtis dissimilarity matrices. A threshold of 50% (black line) distinguishes the dominance of stochastic (> 50%) or deterministic (< 50%) processes. Error bars represent the standard deviation of each process's relative contribution (n = 21). Treatments: control (CK), biochar (B), biochar × compost (BC), and compost (C). **C**, **D** Effects of biochar and compost additions on the relative contributions of deterministic processes in bacterial and fungal community assembly. Effect sizes are represented as regression coefficients derived from rescaled response variables (mean = 0, standard deviation = 1) in linear mixed-effects models. Bars indicate the mean ± s.e.m. of the effect sizes. Statistical significance was determined using Wald type II χ^2 tests (n = 42). Differences in effect sizes among the three urban greenspaces were assessed using a post-hoc LSD test following one-way ANOVA (n = 9), and are indicated by uppercase letters. Sites: P: Peking University; H: Haidian Park; C: Changchun Garden. **E** PLS-PM model investigating relationships between background environmental values, microbial community responses, and changes in environmental factors across three urban greenspaces. Environmental factors include key indicators of soil fertility (SOC, TC, TN) and functioning (CO_2 flux). Δ represents the effect sizes of biochar and compost additions on selected variables. Path coefficients were estimated using 1,000 bootstraps, and are displayed alongside each path (see Table S14 for details). Positive and negative effects are shown in red and blue with solid lines indicating significant relationships ($p < 0.050$) and dashed lines representing non-significant relationships. Explanatory power is provided for each latent variable, and model goodness-of-fit was assessed (> 0.70). **F** Standardized direct, indirect, and total effects (sum of direct and indirect effects) of each variable on the effect sizes of treatment on environmental factors. Significance levels are indicated as: *** $p < 0.001$, ** $p < 0.01$, * $p < 0.05$, # $p < 0.1$

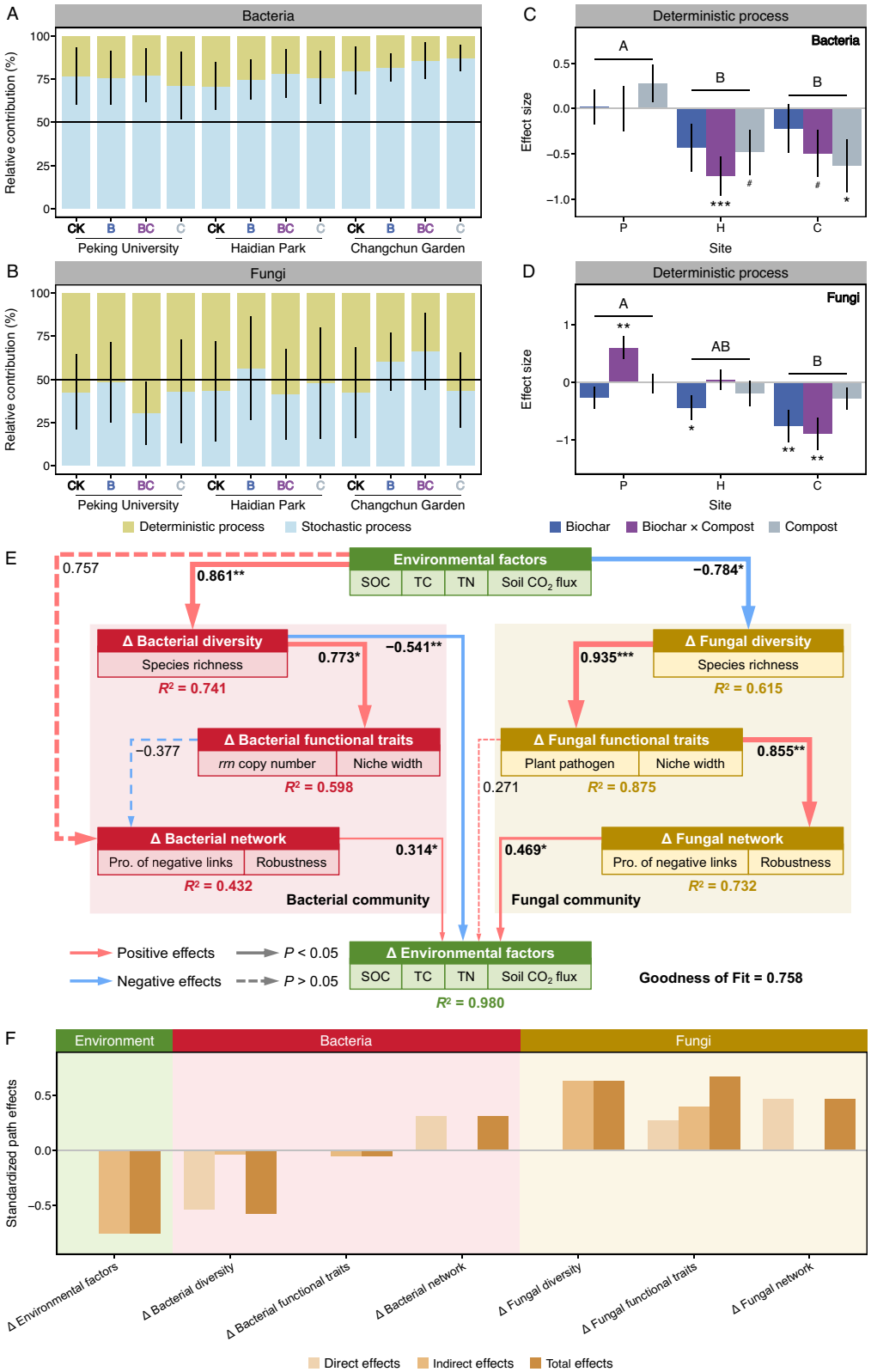

Fig. 6 (See legend on previous page.)

properties ($b = 0.314$, $p = 0.029$), and fungal network properties ($b = 0.469$, $p = 0.03$; Fig. 6E). Overall, these variables accounted for 98.0% of the variation in the effect sizes of treatments on soil fertility and functioning process (Fig. 6E). Additionally, PLS-PM analysis revealed that the effect sizes of treatment on fungal community richness and functional traits exhibited the strongest microbial community-driven influence on responses of environmental factors to treatments (standardized total coefficient = 0.629 to 0.672; Fig. 6F).

4 Discussion

4.1 Specific fungal and bacterial taxa associated with contrasting ecological outcomes

Soil microbial diversity plays a crucial role in supporting the multifunctionality of urban greenspaces (Fan et al. 2023). Soil bacteria are often classified as *r*-strategists characterized by the consumption of labile C compounds, while soil fungi are often classified as *k*-strategists that are more adapted to nutrient-poor niches and exhibit higher efficiency in mineralizing recalcitrant C (Hartman et al. 2017; Yang et al. 2023). Moreover, mycorrhizal fungi contribute to long-term nutrient retention and soil carbon storage through mutualistic exchanges with host plants (Averill et al. 2014; Terrer et al. 2016). Consistently, we observed that treatment-induced increases in TC and TN contents were positively correlated with enhanced soil fungal richness and the fungal-to-bacterial richness ratio (Fig. 2), which were also linked to increased connectivity and stability of the fungal network, but not the bacterial network (Fig. 5). Unlike natural ecosystems, urban greenspaces harbor a significantly higher proportion of Proteobacteria, Ascomycota (including Sordariomycetes, and Leotiomycetes), and plant pathogenic fungi (Delgado-Baquerizo et al. 2021). These microbial groups also emerge as critical mediators of soil responses to organic amendments. For instance, Proteobacteria, typically fast-growing taxa favored by urban fertilization and irrigation regimes (Delgado-Baquerizo et al. 2021; Yang et al. 2023), exhibited an inverse relationship between richness increases and TN accumulation and CO_2 emission (Fig. 3). Plant pathogenic fungi, primarily Sordariomycetes, exhibited a positive correlation with increased TC and TN accumulation in urban greenspaces, likely via inhibiting nutrient uptake by above-ground plants (Fig. 3, 4). In contrast, Leotiomycetes, a group of saprotrophic fungi dependent on exogenous nutrient inputs (Case et al. 2025), were associated with reduced SOC, TC, and TN accumulation and higher CO_2 emission following treatment (Fig. 3, and Fig. S8). Compared to the bacterial community, the fungal community harbored a substantially greater number of taxa linked to positive treatment outcomes for soil TC and TN contents (Fig. 3, and Fig. S8), reinforcing that fungal community played a more pivotal role in maximizing the ecological benefits of organic amendments in urban greenspaces.

4.2 Deterministic role of fungi in response to organic amendments

Contrary to our initial hypothesis, the combined treatment did not achieve the highest carbon sequestration and fertility enhancement effects. Rather, the observed effects were merely the average of the two single additions, or even antagonistic, particularly at the nutrient-rich Changchun Garden (Fig. 1). One plausible explanation is that biochar and compost share a similar fungal community dominated by Eurotiomycetes, while their bacterial communities differ substantially in that biochar stimulates Proteobacteria but compost stimulates Firmicutes (Fig. S7). Since soil nutrient retention is primarily driven by fungal-mediated nutrient uptake from the soil and aboveground plants (Averill et al. 2014; Case et al. 2025), the functional similarity of fungal communities across amendments may tend to exhibit an additive rather than a synergistic effect. Contrary to the predicted "Matthew Effect," where nutrient-rich environments amplify positive responses, carbon sequestration and fertility enhancement were more pronounced in nutrient-poor urban greenspaces (Fig. 1). This observation aligns with findings from the application of biochar and compost in agricultural soils (Yang et al. 2025). The underlying mechanism may be attributed to the more pronounced enhancement of soil microbial activity in less fertile soils compared to fertile ones (Mikajlo et al. 2024). Our field experiments in urban green spaces further elucidated microbial responses, revealing that nutrient-rich environments favor fast-growing species with high *rrn* copy numbers, thereby intensifying microbial competition for resources (Fig. 4). The intensified bacterial resource consumption, coupled with the instability in fungal community composition and function, offset the treatment effect sizes on nutrient gains in nutrient-rich urban greenspaces. In contrast, urban greenspaces with lower background nutrient content (i.e., Peking University and Haidian Park) exhibited higher gains in soil nutrients under treatments, with effect magnitudes ranging from 0.1–14.4 times for SOC, 2.3–2.9 times for TC, and 1.6–2.6 times for TN (Fig. 1). Moreover, the effects of different treatments across various urban greenspaces on soil physicochemical properties and microbial indices showed minimal temporal variation, as indicated by insignificant Treatment × Sampling Time interactions ($p > 0.05$), which suggests that the implemented protective measures contribute to sustained enhancements in carbon sequestration and soil fertility.

5 Conclusion

Biochar and compost amendments are increasingly applied to restore degraded soils and enhance ecosystem services in agroecological systems, yet their effects on soil properties and microbial mechanisms in urban greenspaces remain insufficiently understood. Through a field experiment across three urban greenspaces with contrasting intrinsic soil nutrient levels, this study demonstrates that the outcomes of biochar and compost amendments are strongly nutrient-dependent. Specifically, soil C and N storage was enhanced by amendments, with effects up to 14.4-fold greater in nutrient-poor soils compared to nutrient-rich sites. Mechanistically, in nutrient-poor greenspaces, amendments elevated fungal richness, functional traits, and network connectivity and stability, thereby amplifying soil carbon sequestration and fertility gains. In contrast, nutrient-rich soils exhibited declines in fungal diversity and network stability, accompanied by enhanced bacterial growth and reduced fungal-to-bacterial richness ratios, which collectively accelerated carbon consumption and destabilized soil C pools. Our results highlight fungi as pivotal actors in mediating the ecological benefits of organic amendments, providing a microbial-based conceptual model for precision soil restoration in urban ecosystems. Beyond revealing the contrasting microbial mechanisms across nutrient gradients, this study emphasizes the need to prioritize nutrient-poor urban greenspaces for biochar and compost interventions, where the ecological payoffs are greatest.

Supplementary Information

The online version contains supplementary material available at https://doi.org/10.1007/s42773-026-00599-8.

Supplementary Material 1.

Author contributions

All authors contributed intellectual input and assistance to this study. Qun Gao, Ling Han, and Xin Tong initiated the project. Field management, sample collection, and soil physicochemical and microbial characterization were carried out by Qun Gao, Ling Han, Wenrui Shen, Anqi Liu, Sihang Deng, and Hongkwan Lee. Data analyses were performed by Sihang Deng, who also drafted the manuscript with input from Qun Gao, Ling Han, Zhencheng Ye, Suo Liu, Ke Sun, Xinghui Xia, and Yunfeng Yang. All authors reviewed the results and provided feedback on the manuscript.

Funding

This work was supported by the National Science Foundation for Distinguished Young Scholars (42125703), the National Natural Science Foundation of China (grant numbers T2421005, 42577254, 72061137071), and the Fundamental Research Funds for the Central Universities (2233200009).

Data availability

All data supporting the findings of this study are available in the main text or the Supporting Information. Raw sequences of 16S rRNA gene and ITS amplicons are publicly available in the NCBI SRA database under accession number PRJNA1268377. The database used for *rrn* copy number estimation is publicly available online at https://rrndb.umms.med.umich.edu/downloads/. R scripts for statistical analyses and the relevant datasets are available on GitHub at https://github.com/Deng-Sihang/Urban_greenspace.

Declarations

Competing interests

The authors declare no competing interests.

Author details

[1]School of Environment, Tsinghua University, Beijing 100084, China. [2]Key Laboratory of Water and Sediment Sciences of Ministry of Education, State Key Laboratory of Water Environment Simulation, School of Environment, Beijing Normal University, Beijing 100875, China. [3]College of Environmental Sciences and Engineering, Peking University, Beijing 100871, China. [4]College of Urban and Environmental Sciences, Peking University, Beijing 100871, China. [5]Institute of Environment and Ecology, Tsinghua Shenzhen International Graduate School, Tsinghua University, Shenzhen 518055, China.

Received: 29 August 2025 Revised: 22 February 2026 Accepted: 25 February 2026
Published online: 26 March 2026

References

Averill C, Turner BL, Finzi AC (2014) Mycorrhiza-mediated competition between plants and decomposers drives soil carbon storage. Nature 505(7484):543–545

Bates D, Machler M, Bolker BM, Walker SC (2015) Fitting linear mixed-effects models using lme4. J Stat Softw 67(1):1–48

Broido AD, Clauset A (2019) Scale-free networks are rare. Nat Commun 10:1–10

Case NT, Gurr SJ, Fisher MC, Blehert DS, Boone C, Casadevall A, Chowdhary A, Cuomo CA, Currie CR, Denning DW, Ene IV, Fritz-Laylin LK, Gerstein AC, Gow NAR, Gusa A, Iliev ID, James TY, Jin H, Kahmann R, Klein BS, Kronstad JW, Ost KS, Peay KG, Shapiro RS, Sheppard DC, Shlezinger N, Stajich JE, Stukenbrock EH, Taylor JW, Wright GD, Cowen LE, Heitman J, Segre JA (2025) Fungal impacts on Earth's ecosystems. Nature 638(8049):49–57

Charlop-Powers Z, Pregitzer CC, Lemetre C, Ternei MA, Maniko J, Hover BM, Calle PY, McGuire KL, Garbarino J, Forgione HM, Charlop-Powers S, Brady SF (2016) Urban park soil microbiomes are a rich reservoir of natural product biosynthetic diversity. Proc Natl Acad Sci USA 113(51):14811–14816

Chen L, Jiang Y, Liang C, Luo Y, Xu Q, Han C, Zhao Q, Sun B (2019) Competitive interaction with keystone taxa induced negative priming under biochar amendments. Microbiome 7(1):77

Chen Y, Sun K, Yang Y, Gao B, Zheng H (2024) Effects of biochar on the accumulation of necromass-derived carbon, the physical protection and microbial mineralization of soil organic carbon. Crit Rev Environ Sci Technol 54(1):39–67

Csardi G, Nepusz T (2006) The igraph software package for complex network research. Inter J Complex Syst 1695(5):1–9

Dai Z, Xiong X, Zhu H, Xu H, Leng P, Li J, Tang C, Xu J (2021) Association of biochar properties with changes in soil bacterial, fungal and fauna communities and nutrient cycling processes. Biochar 3(3):239–254

Dai TJ, Wen DH, Bates CT, Wu LW, Guo X, Liu S, Su YF, Lei JS, Zhou JZ, Yang YF (2022) Nutrient supply controls the linkage between species abundance and ecological interactions in marine bacterial communities. Nat Commun 13(1):1–9

Delgado-Baquerizo M, Eldridge DJ, Liu Y-R, Sokoya B, Wang J-T, Hu H-W, He J-Z, Bastida F, Moreno JL, Bamigboye AR, Blanco-Pastor JL, Cano-Díaz C, Illán JG, Makhalanyane TP, Siebe C, Trivedi P, Zaady E, Verma JP, Wang L, Wang J, Grebenc T, Peñaloza-Bojacá GF, Nahberger TU, Teixido AL, Zhou X-Q, Berdugo M, Duran J, Rodríguez A, Zhou X, Alfaro F, Abades S, Plaza C, Rey A, Singh BK, Tedersoo L, Fierer N (2021) Global homogenization of the structure and function in the soil microbiome of urban greenspaces. Sci Adv 7(28):eabg5809

Delgado-Baquerizo M, García-Palacios P, Bradford MA, Eldridge DJ, Berdugo M, Sáez-Sandino T, Liu Y-R, Alfaro F, Abades S, Bamigboye AR, Bastida F, Blanco-Pastor JL, Duran J, Gaitan JJ, Illán JG, Grebenc T, Makhalanyane TP, Jaiswal DK, Nahberger TU, Peñaloza-Bojacá GF, Rey A, Rodríguez A, Siebe

C, Teixido AL, Sun W, Trivedi P, Verma JP, Wang L, Wang J, Yang T, Zaady E, Zhou X, Zhou X-Q, Plaza C (2023) Biogenic factors explain soil carbon in paired urban and natural ecosystems worldwide. Nat Clim Chang 13(5):450–455

Edgar RC (2018) Updating the 97% identity threshold for 16S ribosomal RNA OTUs. Bioinformatics 34(14):2371–2375

Fairbairn AJ, Meyer ST, Mühlbauer M, Jung K, Apfelbeck B, Berthon K, Frank A, Guthmann L, Jokisch J, Kerler K, Müller N, Obster C, Unterbichler M, Webersberger J, Matejka J, Depner P, Weisser WW (2024) Urban biodiversity is affected by human-designed features of public squares. Nature Cities 1:706–715

Fan KK, Chu HY, Eldridge DJ, Gaitan JJ, Liu YR, Sokoya B, Wang JT, Hu HW, He JZ, Sun W, Cui HY, Alfaro FD, Abades S, Bastida F, Diaz-López M, Bamigboye AR, Berdugo M, Blanco-Pastor JL, Grebenc T, Duran J, Illán JG, Makhalanyane TP, Mukherjee A, Nahberger TU, Penaloza-Bojaca GF, Plaza C, Verma JP, Rey A, Rodriguez A, Siebe C, Teixido AL, Trivedi P, Wang L, Wang JY, Yang TX, Zhou XQ, Zhou XB, Zaady E, Tedersoo L, Delgado-Baquerizo M (2023) Soil biodiversity supports the delivery of multiple ecosystem functions in urban greenspaces. Nat Ecol Evol 7(1):113–126

Giardine B, Riemer C, Hardison RC, Burhans R, Elnitski L, Shah P, Zhang Y, Blankenberg D, Albert I, Taylor J, Miller W, Kent WJ, Nekrutenko A (2005) Galaxy: a platform for interactive large-scale genome analysis. Genome Res 15(10):1451–1455

Gu B, Zhang X, Lam SK, Yu Y, van Grinsven HJM, Zhang S, Wang X, Bodirsky BL, Wang S, Duan J, Ren C, Bouwman L, de Vries W, Xu J, Sutton MA, Chen D (2023) Cost-effective mitigation of nitrogen pollution from global croplands. Nature 613(7942):77–84

Guo H, Du E, Terrer C, Jackson RB (2024) Global distribution of surface soil organic carbon in urban greenspaces. Nat Commun 15(1):806

Hartman WH, Ye R, Horwath WR, Tringe SG (2017) A genomic perspective on stoichiometric regulation of soil carbon cycling. ISME J 11(12):2652–2665

Kembel SW, Cowan PD, Helmus MR, Cornwell WK, Morlon H, Ackerly DD, Blomberg SP, Webb CO (2010) Picante: R tools for integrating phylogenies and ecology. Bioinformatics 26(11):1463–1464

Lee ZMP, Bussema C, Schmidt TM (2009) rrnDB: documenting the number of rRNA and tRNA genes in bacteria and archaea. Nucl Acid Res 37:D489–D493

Lehmann J, Cowie A, Masiello CA, Kammann C, Woolf D, Amonette JE, Cayuela ML, Camps-Arbestain M, Whitman T (2021) Biochar in climate change mitigation. Nat Geosci 14(12):883–892

Levins R (1968) Evolution in changing environments: some theoretical explorations. Princeton University Press. https://doi.org/10.2307/j.ctvx5wbbh

Li C, Chen X, Jia Z, Zhai L, Zhang B, Grüters U, Ma S, Qian J, Liu X, Zhang J, Müller C (2024) Meta-analysis reveals the effects of microbial inoculants on the biomass and diversity of soil microbial communities. Nat Ecol Evol 8(7):1270–1284

Liang Y, Ning D, Lu Z, Zhang N, Hale L, Wu L, Clark IM, McGrath SP, Storkey J, Hirsch PR, Sun B, Zhou J (2020) Century long fertilization reduces stochasticity controlling grassland microbial community succession. Soil Biol Biochem 151:108023

Ling J, Dungait JAJ, Delgado-Baquerizo M, Cui Z, Zhou R, Zhang W, Gao Q, Chen Y, Yue S, Kuzyakov Y, Zhang F, Chen X, Tian J (2025) Soil organic carbon thresholds control fertilizer effects on carbon accrual in croplands worldwide. Nat Commun 16(1):3009

Long X, Li J, Liao X, Wang J, Zhang W, Wang K, Zhao J (2025) Stable soil biota network enhances soil multifunctionality in agroecosystems. Glob Chang Biol 31(1):e70041

Luo S, Han J, Chen R, Delgado-Baquerizo M, Zhang W, Feng Y (2024) Impact of socioeconomic factors on soil-borne animal pathogenic fungi in urban greenspaces. Nat Cities 1:406–412

Merton RK (1968) The Matthew effect in science. Science 159(3810):56–63

Mikajlo I, Lerch TZ, Louvel B, Hynšt J, Záhora J, Pourrut B (2024) Composted biochar versus compost with biochar: effects on soil properties and plant growth. Biochar 6(1):85

Montesinos-Navarro A, Hiraldo F, Tella JL, Blanco G (2017) Network structure embracing mutualism-antagonism continuums increases community robustness. Nat Ecol Evol 1(11):1661–1669

Nan Q, Speth DR, Qin Y, Chi W, Milucka J, Gu B, Wu W (2025) Biochar application using recycled annual self straw reduces long-term greenhouse gas emissions from paddy fields with economic benefits. Nat Food 6(5):456–465

Ning DL, Deng Y, Tiedje JM, Zhou JZ (2019) A general framework for quantitatively assessing ecological stochasticity. Proc Natl Acad Sci U S A 116(34):16892–16898

Põlme S, Abarenkov K, Henrik Nilsson R, Lindahl BD, Clemmensen KE, Kauserud H, Nguyen N, Kjøller R, Bates ST, Baldrian P, Frøslev TG, Adojaan K, Vizzini A, Suija A, Pfister D, Baral H-O, Järv H, Madrid H, Nordén J, Liu J-K, Pawlowska J, Põldmaa K, Pärtel K, Runnel K, Hansen K, Larsson K-H, Hyde KD, Sandoval-Denis M, Smith ME, Toome-Heller M, Wijayawardene NN, Menolli N, Reynolds NK, Drenkhan R, Maharachchikumbura SSN, Gibertoni TB, Læssøe T, Davis W, Tokarev Y, Corrales A, Soares AM, Agan A, Machado AR, Argüelles-Moyao A, Detheridge A, de Meiras-Ottoni A, Verbeken A, Dutta AK, Cui B-K, Pradeep CK, Marín C, Stanton D, Gohar D, Wanasinghe DN, Otsing E, Aslani F, Griffith GW, Lumbsch TH, Grossart H-P, Masigol H, Timling I, Hiiesalu I, Oja J, Kupagme JY, Geml J, Alvarez-Manjarrez J, Ilves K, Loit K, Adamson K, Nara K, Küngas K, Rojas-Jimenez K, Bitenieks K, Irinyi L, Nagy LG, Soonvald L, Zhou L-W, Wagner L, Aime MC, Öpik M, Mujica MI, Metsoja M, Ryberg M, Vasar M, Murata M, Nelsen MP, Cleary M, Samarakoon MC, Doilom M, Bahram M, Hagh-Doust N, Dulya O, Johnston P, Kohout P, Chen Q, Tian Q, Nandi R, Amiri R, Perera RH, dos Santos Chikowski R, Mendes-Alvarenga RL, Garibay-Orijel R, Gielen R, Phookamsak R, Jayawardena RS, Rahimlou S, Karunarathna SC, Tibpromma S, Brown SP, Sepp S-K, Mundra S, Luo Z-H, Bose T, Vahter T, Netherway T, Yang T, May T, Varga T, Li W, Coimbra VRM, de Oliveira VRT, de Lima VX, Mikryukov VS, Lu Y, Matsuda Y, Miyamoto Y, Kõljalg U, Tedersoo L (2020) FungalTraits: a user-friendly traits database of fungi and fungus-like stramenopiles. Fungal Divers 105(1):1–16

Reyes-Torres M, Oviedo-Ocaña ER, Dominguez I, Komilis D, Sánchez A (2018) A systematic review on the composting of green waste: feedstock quality and optimization strategies. Waste Manag 77:486–499

Roller BRK, Stoddard SF, Schmidt TM (2016) Exploiting rRNA operon copy number to investigate bacterial reproductive strategies. Nat Microbiol 1(11):16160

Ruan Q, Dutta D, Schwalbach MS, Steele JA, Fuhrman JA, Sun F (2006) Local similarity analysis reveals unique associations among marine bacterioplankton species and environmental factors. Bioinformatics 22(20):2532–2538

Salazar G (2015) EcolUtils: utilities for community ecology analysis. R package ver. 0.1

Sanchez G (2013) PLS path modeling with R. Berkeley Trowchez Edit 383(2013):551

Singh H, Northup BK, Rice CW, Prasad PVV (2022) Biochar applications influence soil physical and chemical properties, microbial diversity, and crop productivity: a meta-analysis. Biochar 4(1):8

Terrer C, Vicca S, Hungate BA, Phillips RP, Prentice IC (2016) Mycorrhizal association as a primary control of the CO_2 fertilization effect. Science 353(6294):72–74

Tian L, Wang Y, Jin D, Zhou Y, Mukhamed B, Liu D, Feng B (2025) The application of biochar and organic fertilizer substitution regulates the diversities of habitat specialist bacterial communities within soil aggregates in proso millet farmland. Biochar 7(1):6

Weiss S, Van Treuren W, Lozupone C, Faust K, Friedman J, Deng Y, Xia LC, Xu ZZ, Ursell L, Alm EJ, Birmingham A, Cram JA, Fuhrman JA, Raes J, Sun FZ, Zhou JZ, Knight R (2016) Correlation detection strategies in microbial data sets vary widely in sensitivity and precision. ISME J 10(7):1669–1681

Wilson B, Hayek L-AC (2015) Distinguishing relative specialist and generalist species in the fossil record. Mar Micropaleontol 119:7–16

Wu J, Barahona M, Tan YJ, Deng HZ (2010) Natural connectivity of complex networks. Chin Phys Lett 27:7

Wu LY, Wen CQ, Qin YJ, Yin HQ, Tu QC, Van Nostrand JD, Yuan T, Yuan MT, Deng Y, Zhou JZ (2015) Phasing amplicon sequencing on Illumina Miseq for robust environmental microbial community analysis. BMC Microbiol 15:125

Wu S, Chen B, Webster C, Xu B, Gong P (2023) Improved human greenspace exposure equality during 21st century urbanization. Nat Commun 14(1):6460

Yang Y, Dou Y, Wang B, Xue Z, Wang Y, An S, Chang SX (2023) Deciphering factors driving soil microbial life-history strategies in restored grasslands. iMeta 2(1):e66

Yang J, Xia L, van Groenigen KJ, Zhao X, Ti C, Wang W, Du Z, Fan M, Zhuang M, Smith P, Lal R, Butterbach-Bahl K, Han X, Meng J, Liu J, Cai H, Cheng Y, Liu X, Shu X, Jiao X, Pan Z, Tang G, Yan X (2025) Sustained benefits of

long-term biochar application for food security and climate change mitigation. Proc Natl Acad Sci U S A 122(33):e2509237122
Yuan MM, Guo X, Wu LW, Zhang Y, Xiao NJ, Ning DL, Shi Z, Zhou XS, Wu LY, Yang YF, Tiedje JM, Zhou JZ (2021) Climate warming enhances microbial network complexity and stability. Nat Clim Chang 11(4):343–348
Zhou JZ, Bruns MA, Tiedje JM (1996) DNA recovery from soils of diverse composition. Appl Environ Microbiol 62(2):316–322
Zhou X, Feng Z, Yao Y, Liu R, Shao J, Jia S, Gao Y, Xue K, Chen H, Fu Y, He Y (2025) Nitrogen input alleviates the priming effects of biochar addition on soil organic carbon decomposition. Soil Biol Biochem 202:109689